6th International Symposium on Space Sailing (ISSS 2023), New York, USA, 5-9 June 2023

A Solar Sail Shape Modeling Approach for Attitude Control Design and Analysis

Benjamin M. GAUVAIN[a,*], Daniel A. TYLER[a]

[a]*NASA Marshall Space Flight Center, Huntsville, Alabama, USA*

Abstract

Solar sails operating in the space environment experience deformations in sail shape that result in relatively large disturbance torques which dictate the required performance of the spacecraft attitude control and momentum management systems. These deformations are driven by thermal loads on the booms (due to uneven solar heating), manufacturing and assembly tolerances, and variations in membrane tension. The Solar Cruiser spacecraft utilizes a four-quadrant sail design with four 30-meter length booms and four triangular sail membranes, creating a square sail structure of >1600 m^2. Medium-fidelity mesh models were developed based on a characteristic deformed shape. A series of parametric studies were conducted using this shape paradigm to determine worst-case deformed sail shapes which produce bounding disturbance torques. A large database of shapes was produced, and the forces and moments induced by each individual shape were calculated using a Rios-Reyes reduced order generalized sail model [1]. Two were selected as reference worst-case shapes for the Solar Cruiser mission: one which produced the highest pitch/yaw root-sum-squared (RSS) torque, and one which produced the highest roll torque. The results showed that the worst-case shapes at high solar incidence angles induce significantly higher (2-10x) disturbance torques than an ideal, flat-plate sail. Even with considerable safety margins, assuming an ideal sail is unlikely to sufficiently bound the disturbances, which is critical when designing the attitude control system and sizing actuators. Accurate sail shape modeling methodologies should therefore be employed on future solar sail missions.

Keywords: Solar, Sail, Model, Attitude, Control

Nomenclature

AMT	Active Mass Translator
CM	Center of Mass
CP	Center of Pressure
FEEP	Field Emission Electric Propulsion
FEM	Finite Element Model
IFM	Indium FEEP Micro-thrusters
NEA	Near-Earth Asteroid
PDLC	Polymer-Dispersed Liquid Crystal
RCD	Reflectivity Control Device
RCS	Reaction Control System
RW	Reaction Wheel
SIA	Solar Incidence Angle
SRP	Solar Radiation Pressure
$\tilde{r}$	total reflectivity
s	specular reflectivity fraction
Bf	front side non-Lambertian coefficient
Bb	back side non-Lambertian coefficient
ef	front side emissivity
eb	back side emissivity

1. Introduction

SRP-induced disturbance torques are a major design driver for solar sails, impacting the architecture and design of the attitude control system, including control actuators and momentum management actuators. Traditionally, CM/CP offset of a flat sail has been the primary or sole metric for predicting disturbance torques and sizing systems accordingly [2]. However, it was discovered during development of the NEA Scout mission that deformed sail shape effects were a significant contributor to the overall SRP-induced disturbance torques [3]. A mesh model of the sail produced from a structural FEM was transformed into a reduced-order Rios-Reyes/Scheeres generalized sail tensor model [1] to efficiently calculate the forces and torques on the sail at varying sun-relative attitudes which resulted in a significant increase in the predicted magnitude of disturbance torques, especially about the roll axis, under worst-case conditions. The NEA Scout

* Corresponding author, benjamin.m.gauvain@nasa.gov

model was scaled and adapted for Solar Cruiser with the addition of further sail shape model manipulations to capture boom tip deflections and uncertainties specific to the Solar Cruiser sail.

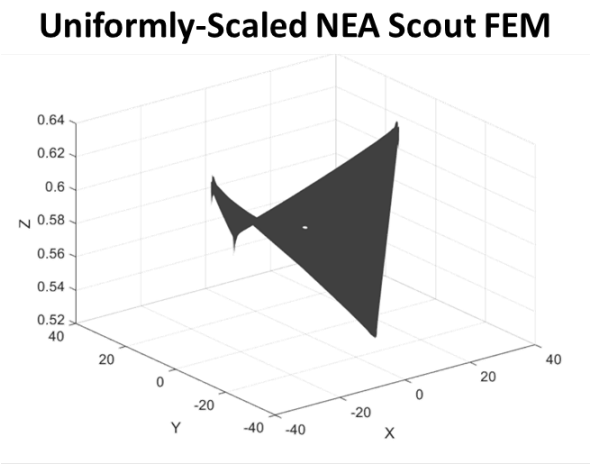

Figure 1. Scaled NEA Scout Deformed Sail Model

This process uncovered additional sensitivities of the disturbance torques to characteristics of the sail shape, namely the impact of boom tip deflection uncertainty on disturbance torques. It also showed that out-of-plane tip deflections were the biggest driver of disturbance torques, inducing magnitudes >5x for a flat sail of identical dimensions, and >2x for an identical sail with in-plane tip deflections only.

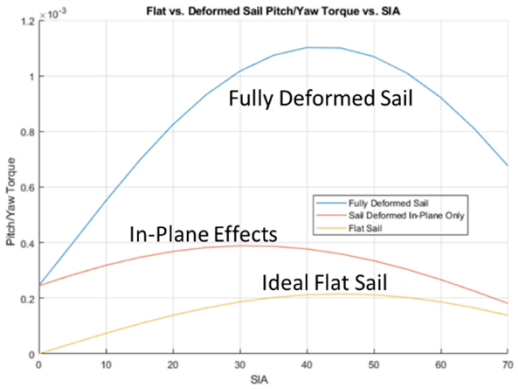

Figure 2. Dist. Torque Comparison, Scaled NEA Scout Model

However, this shape modeling approach was still fairly limited in flexibility and fidelity, given that it merely involved scaling the NEA Scout model, and left a lot of uncertainty in its ability to bound the problem. Thus, a more detailed approach was developed and implemented for Solar Cruiser that involves a wide parametric sweep over several key design parameters, predominantly related to sail shape, to improve the likelihood that the predicted disturbance torques are properly bounded during development.

2. Methodology

2.1. Process Overview

The strongest determinant of the sail shape is the deflection of each of the four booms. By far the largest known and predictable effect on boom deflections is the thermal gradient across the booms in the out-of-plane direction, from the sun-facing side (front) to the space-facing side (back). The resulting boom deflections, measured at the tip for simplicity, define the "nominal" sail shape which is used to create the initial deformed sail mesh before applying uncertainty/error terms. For Solar Cruiser, thermal analyses were conducted at various representative attitudes, including 0 to 17 degrees SIA (the range for its mission profile) with both "corner-on" and "edge-on" rotations, or clock angles of 0 and 45 degrees, respectively. The resulting thermal loads were applied to a structural FEM, and the resulting boom tip deflections were captured and tabulated. The case with the largest average boom tip deflections was chosen for conservatism.

With the nominal boom tip deflections defined, it was then necessary to identify other possible uncertainty/error terms. The uncertainties selected for this study include boom tip error, membrane deflections, and center of mass offsets, as described in Table 1.

Table 1. Deformation Uncertainty Parameter Descriptions

Parameter	Description
Membrane Deflections	Out-of-plane, billowing shape with peak/trough at the centroid of each quadrant. The magnitude was varied, and the direction varied in the sail out-of-plane axis.
Nominal Boom Tip Deflections	Out-of-plane, increasing parabolically from root to tip. The magnitude and direction (out of the sail plane and toward the sun) were held constant.
Boom Tip Deflection Errors	Random/uncertain out-of-plane boom tip deflections due to manufacturing and assembly tolerances, tension changes in the membrane, and thermal load uncertainties. The magnitude was varied, and the direction varied in the sail out-of-plane axis.
In-Plane Center of Mass (CM) Offsets	The difference in the center of mass in-plane position with the AMT homed relative to the designed geometric center, due to manufacturing and assembly tolerances.
Attitude	SIA varied from 0 to 17 degrees (target for Plane Change Demonstration) and clock angle varied from 0 to 360 degrees.

The parameter variations for these uncertainty terms are summarized in Table 2. Membrane deflections of up to 5 cm at the quadrant centroid were chosen as the maximum billowing amount, while tip error was varied

up to a 100% increase for conservatism. The maximum CM offset magnitude is based on sail manufacturability and was determined through discussion with the solar sail system prime contractor. All boom tip deflections were applied in the out-of-plane (z-axis/roll) direction only, to reduce model complexity; previous modeling efforts had shown (Fig. 2) that in-plane (x-axis/pitch, y-axis/yaw) deflections have a significantly smaller impact on disturbance torques compared to out-of-plane deflections. It is also expected that modeling membrane billowing will capture the reduced tension occurring across a quadrant from two booms deflecting closer relative to each other.

Table 2. Deformation Uncertainty Parameter Variations

Parameter	Tip Error Factor	Mem. Billow	CM Offset	Tip Direction Factor	Mem. Direction Factor
Variation	0	0 cm	0 cm	1x	-1x
	1x	1 cm	+/-1 cm X-axis	Tip A +/-1x	Membrane A +/-1x
	1.25x	2 cm	+/-2 cm X-axis	Tip B +/-1x	Membrane B +/-1x
	1.5x	3 cm	+/-1 cm Y-axis	Tip C +/-1x	Membrane C +/-1x
	1.75x	4 cm	+/-2 cm Y-axis	Tip D +/-1x	Membrane D +/-1x
	2.0x	5 cm	-	-	-

Deformed sail mesh models were created by modifying a flat sail mesh according to shape functions and geometric boundary conditions summarized in Table 1 and detailed in Section 2.2. A large parametric sweep was then conducted over uncertainty/error terms, with each combination producing a mesh model. This produced a large database of mesh models, all of which were transformed into a reduced-order Rios-Reyes generalized sail tensor model [1], as with NEA Scout. Finally, the SRP-induced forces and torques were calculated across the range of Solar Cruiser sun-relative mission attitudes, which included clock angle variations of 0 to 360 degrees and solar incidence angles of 0 to 17 degrees. The sail optical properties used for force and torque calculations were determined from prior NEA Scout optical testing conducted by NASA in 2015 which analyzed the effect of wrinkles on the specular fraction of reflection [3], shown below in Table 3.

Table 3. Reflectivity Coefficients

Coefficient	$\tilde{r}$	s	B_f	B_b	e_f	e_b
Value	0.91	0.89	0.79	0.67	0.025	0.27

Post-processing of the force and torque data was then done to identify two worst-case sail shapes: one which induced the largest pitch/yaw root-sum-squared torque, and one which induced the largest roll torque. Because in-plane disturbance torques are sensitive to different sail deformation parameters than out-of-plane disturbance torques, one deformed shape does not adequately bound both cases. Solar Cruiser utilized separate devices for momentum management in the pitch/yaw axes and roll axis. Sizing and design considerations for each axis are dependent on the maximum disturbance torque associated with the corresponding shape. Therefore, to adequately design the Solar Cruiser control and momentum management actuators, it was necessary to account for both possible shapes. Fig. 3 illustrates the functional process flow of the Solar Cruiser modeling methodology.

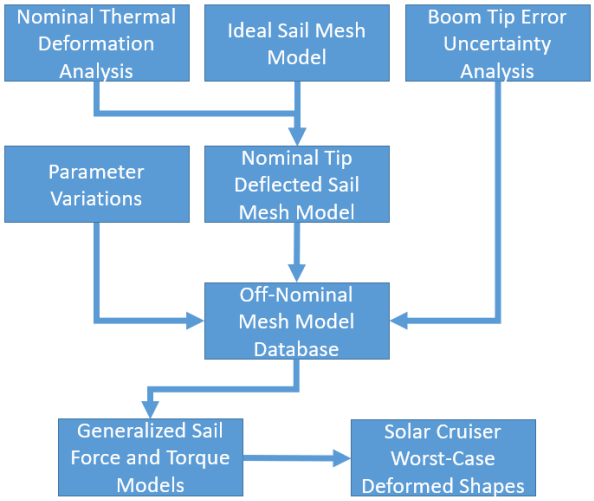

Figure 3. Model Methodology Process Flow

2.2. *Boundary Conditions and Assumptions*

In order to create the database of off-nominal, deformed sail shapes, a flat sail mesh model with Solar Cruiser dimensions was used as the starting point; deformed shapes were synthesized by applying changes to the z-axis location of each point in the mesh according to geometric shape functions with boundary conditions based on expected deformation patterns (e.g., parabolic booms and billowing membranes).

The out-of-plane deflection of a point p on a sail quadrant between booms *i* and *i+1* (where *i* ranges from 1 to 4) can be written as:

$$\Delta z_p = f\left(\mathrm{r}, \theta, \Delta Z_{tip\,i}, \Delta Z_{tip\,i+1}, \Delta Z_{billow,max}\right) \quad (1)$$

The boundary conditions at the edges of each membrane are defined such that they follow a parabolic curve from the centroid of the sailcraft to the tip of the adjoining boom, according to:

$$\Delta z_{edge\,i}(r) = \Delta Z_{tip\,i} \left(\frac{r}{L}\right)^2 \quad (2)$$

Where r is the radial distance from the sailcraft centroid of a point along the edge and L is the total length of the edge. The parabolic curve is chosen due to its conservatism indicated in an early sensitivity study comparing linear and quadratic deflections vs. radial distance.

The out-of-plane deflections for a point p on the membrane resulting from the boom boundary conditions, disregarding billowing effects, is derived by interpolating between the two edges along curves of constant radial distance from the centroid, as follows:

$$\Delta z_{p,base}(r,\theta) = \Delta Z_{tip\,i}\left(\frac{r}{L}\right)^2 + \frac{\theta-\theta_{edge\,i}}{\theta_{edge\,i+1}-\theta_{edge\,i}}\left(\Delta Z_{tip\,i+1} - \Delta Z_{tip\,i}\right)\left(\frac{r}{L}\right)^2 \quad (3)$$

$$\Rightarrow \Delta z_{p,base}\left(r,\theta_{edge\,i}\right) = \Delta z_{edge\,i}(r) \quad (4)$$

$$\Delta z_{p,base}\left(r,\theta_{edge\,i+1}\right) = \Delta z_{edge\,i+1}(r) \quad (5)$$

Finally, the effect of billowing is added using a boundary condition to constrain the out-of-plane billowing at the centroid of the triangular sail quadrant – located along the line from the vertex at the sailcraft centroid to the midspan of the distal edge, 2/3 of this length from the vertex – to be equal to the maximum billowing deflection magnitude for that membrane. The shape of the membrane out-of-plane deflection due to billowing smoothly connects this membrane centroid location to the previous defined membrane boundaries and is superimposed on the base deflection ($\Delta z_{p,base}$). This shape is modeled as a two-dimensional sinusoid as a function of radial location, r, and angular location, θ, in polar coordinates in the sail plane, according to Eq. (6) below, given the smooth transition between boundaries. Note, however, that this specific "shape function" is not necessarily reflective of physically realistic shapes.

$$\Delta z_{p,billow}(r,\theta) = \Delta Z_{billow,\max}\left|\sin\left(\frac{r}{\frac{2}{3}\left(\frac{L}{\sqrt{2}}\right)}\frac{\pi}{2}\right)\times \sin\left(\frac{\theta-\theta_{edge\,i}}{\theta_{edge\,i+1}-\theta_{edge\,i}}\pi\right)\right| \quad (6)$$

$$\Rightarrow \Delta z_{p,billow}\left(\frac{2}{3}\left(\frac{L}{\sqrt{2}}\right), \frac{\theta_{edge\,i}+\theta_{edge\,i+1}}{2}\right) = \Delta Z_{billow,\max} \quad (7)$$

Thus, the total out-of-plane deflection of any point on the membrane of the sail is calculated using the expression:

$$\Delta z_p(r,\theta) = \Delta z_{p,base}(r,\theta) + \Delta z_{p,billow}(r,\theta) \quad (8)$$

Other modeling assumptions in addition to the geometric boundary conditions:

- Non-sail membrane surfaces (including shadowing of the sail membranes by such), sail membrane wrinkles (which are not directly modeled, but captured via optical properties), and in-plane deformations or asymmetries of any kind are assumed to contribute a negligible amount to solar forces and torques relative to out-of-plane deflections of the sail membranes and are, therefore, excluded from the sail shape model.
- The sail membranes are modeled with a fixed-fixed interface to the booms at the roots and tips without any separation (e.g., free membrane inner diameter) or interference (e.g., catenary-boom rubbing).
- Boom tips and sail membranes can deflect out of plane in any arbitrary direction with respect to each other. The effect of out-of-plane deformations on the in-plane dimensions of sail elements (due to elongation, relaxation, or obliqueness) is neglected.
- The function used to calculate out-of-plane deformation at a node as a function of in-plane location, given some boom tip and sail membrane deformation magnitudes, is derived with the only constraint being that the boundary conditions dictated by the "fixed-fixed" assumption stated above and the sail membrane deformation magnitudes are met and without regards to any structural modeling.

3. Results and Discussion

3.1. Worst-Case Sail Shape Results

The disturbance torques induced by the Solar Cruiser worst-case shapes are shown in Fig. 4 and 5. Torques are plotted across the range of Solar Cruiser mission design attitudes (clock angles up to 360 degrees and SIA up to 17 degrees). Note that the relationship between torque, SIA, and clock angles inform mission operational considerations; clock angles can be commanded which minimize the induced disturbances while maintaining the required SIA for mission design. Additionally, at higher SIAs, the worst-case roll shape contains a zero crossing where torque can be completely eliminated. The torque curves obtained from this study are due to theoretical shapes; in practice, the efficacy of

clock angle control approaches depends on accurate sail characterization on-orbit after sail deployment.

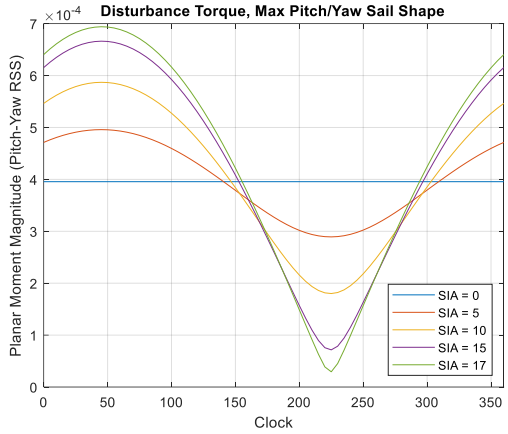

Figure 4. Max Pitch/Yaw Disturbance Torque

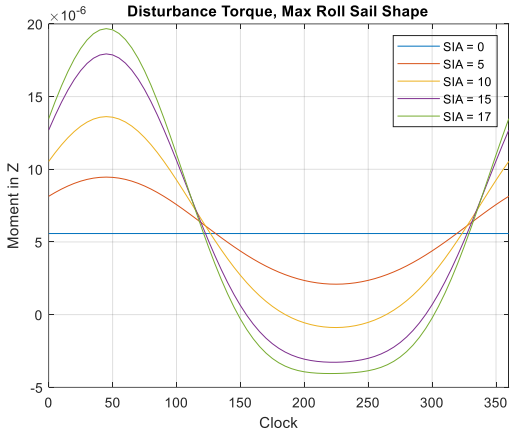

Figure 5. Max Roll Disturbance Torque

Plots of the worst-case sail mesh models are shown below in Fig. 6 and 7. The z-axis scale is amplified to illustrate how the deformations affect global sail shape.

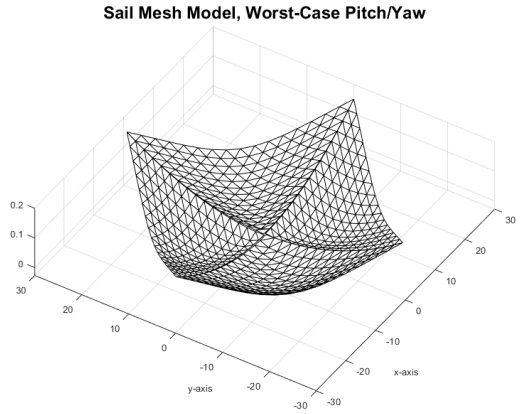

Figure 6. Solar Cruiser Worst-Case Pitch/Yaw Shape

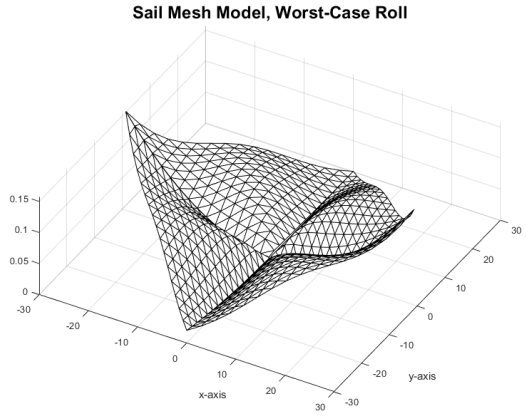

Figure 7. Solar Cruiser Worst-Case Roll Shape

The deformed sail shapes show significantly higher disturbance torques than an ideal flat sail, as shown in Fig. 8 and 9, for the updated medium-fidelity Solar Cruiser shapes. The worst-case maximum roll torque for the characteristic roll shape is a factor of 2.06 higher; this exceeds even the conservative amounts of margin typically carried in the early concept phases of missions. It is worth noting that increasing the model fidelity reduced the expected worst-case disturbance torques compared to the early mission low-fidelity scaled NEA Scout models; however, this was largely driven by increased model fidelity in the thermal analyses resulting in lower nominal boom tip deflections. This benefit was specific to the Solar Cruiser configuration and mission design.

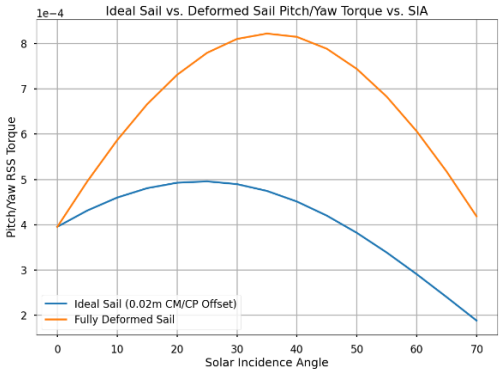

Figure 8. Ideal vs. Deformed Sail Comparison, Pitch/Yaw

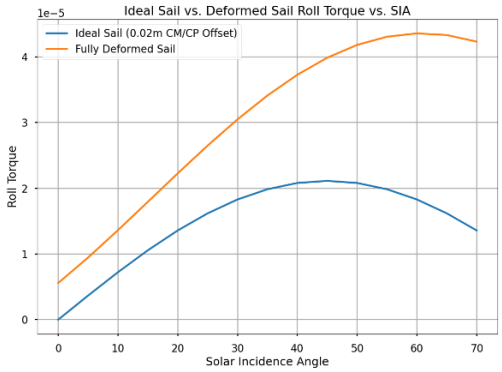

Figure 9. Ideal vs. Deformed Sail Comparison, Roll

3.2. Solar Cruiser Design Considerations

The development of the final worst-case sail models and subsequent torque predictions impacted the Solar Cruiser design and analysis cycle. These models were used to bound the expected SRP-induced disturbance torque. The disturbance torque values affected requirements derivation. Sail shape requirements were determined to ensure the as-manufactured flight sail deformations would remain within the modeled deformations. The predicted disturbance torques were used, in addition to other expected disturbances and slew rate capability requirements, to define the reaction wheel torque capability requirement.

The worst-case pitch/yaw torque predictions were used to define requirements for the momentum management systems. To desaturate momentum in the pitch/yaw (in-plane) axes, Solar Cruiser utilized an AMT, which separates the spacecraft bus from the sail using rails and drive motors, allowing changes in the center of mass with respect to the center of pressure applied to the sail from SRP [4], inducing a torque. The deformed sail disturbance predictions drive design considerations such as AMT range of motion, rail orientation, and bus mass allocation; a higher mass ratio between the bus and sail sides of separation yields better AMT performance.

For roll momentum management, Solar Cruiser utilized two actuator systems: RCDs and IFMs. RCDs contain electroactive PDLC materials which vary reflectivity when a voltage is applied; by orienting the RCDs at a tented angle relative to the sail plane and varying geometrically opposed RCD on/off states, torques about the roll axis can be imparted [4]. The IFMs fulfill the same role as that of a traditional RCS system, allowing RW desaturation in the event of RCD underperformance. Roll torque predictions drive requirements on RCD surface area, as well as IFM/RCS propellant mass needed.

To verify requirements and conduct design and analysis cycles, a sailcraft integrated model was developed which incorporates plant dynamics as well as a control system and flight software model. The worst-case torque predictions were integrated into this model using the Rios-Reyes generalized sail tensors, allowing computationally efficient force and torque calculation at simulated attitudes.

4. Conclusions and Forward Work

4.1. Conclusions

The deformed sail model results demonstrate considerably higher expected induced disturbance torques compared to the simplified assumption of a flat plate sail with a CM/CP offset. Accurate prediction of these disturbances is crucial when designing the spacecraft attitude control system. The reaction wheels (or other primary control actuator) must have sufficient torque capability to achieve a control authority >1, plus program-dependent margin. Similarly, the momentum management system must be sized accordingly. As disturbance torques grow with increasing SIA, more momentum management capacity is needed to prevent RW saturation. If the spacecraft uses an RCS for RW desaturation, this will result in additional propellant mass to meet mission objectives. As all required masses grow (control actuators, momentum management actuators, propellant mass, bus mass) the sailcraft characteristic acceleration decreases. Thus, sail deformations are a significant driver of the mission and sailcraft design. Because of the compounding effect of sail deformations on all aspects of the design, it is recommended to begin medium/high fidelity modeling as early as possible in the design cycle, even in the early mission concept phase.

4.2. Forward Work

The approach detailed in this paper yields a medium-fidelity model where inputs and assumptions on local conditions (e.g., nominal boom tip deflection, tip error uncertainty, and membrane deflection) drive the global sail shape. Forward work is currently ongoing to improve modeling fidelity using a globally-driven, top-down approach. An iterative process will be used where the interactions and interdependencies, especially the nonlinear ones, between the boom deformations and the membrane deformations are increasingly refined through interleaving “global” models driven by the booms and “local” models which represent membrane deformations given some boundary conditions (driven by the boom deformations). Assumed membrane shapes will be replaced with those derived from physics-based modeling with higher-fidelity models of the external and internal loads, material properties, and structural mechanics. This approach also aims to apply uncertainties and tolerances as inputs to the structural FEM so that their effects may be more accurately

captured, as opposed to using simplified models to predict the effects and applying them in post-processing (e.g., boom tip error terms). The end goal of this work is to ultimately obtain a more physically realistic, high-fidelity representation of the actual sail shape.

Acknowledgments

The authors would like to thank the Solar Cruiser Project for the opportunity to conduct this innovative work, as well as providing the funding through which it was completed and this paper was written. Additionally, thanks to Redwire Corporation and ATA Engineering for the solar sail design and modeling inputs used in the sail shape analysis. Thanks to NeXolve Holding Company, LLC, for providing technical data on the sail membrane. Finally, thanks to the NEA Scout project and Guidance and Control team for the knowledge they passed down including previous modeling, analysis, and testing that was used as the basis for the methods detailed in this paper.

References

[1] L. Rios-Reyes and D. J. Scheeres. Generalized Model for Solar Sails. Journal of Spacecraft and Rockets, 42(1):182–185, 2005. doi: 10.2514/1.9054.

[2] B. Wie. Solar Sail Attitude Control and Dynamics, Part 1. Journal of Guidance, Control, and Dynamics, 27(4):526-535, 2004. doi: 10.2514/1.11134.

[3] A. Heaton, N. Ahmad, and K. Miller. Near Earth Asteroid Scout Thrust and Torque Model. Kyoto, Japan, January 2017. International Symposium on Solar Sailing. Paper M17-5721.

[4] D. Tyler, B. Diedrich et al. Attitude Control Approach for Solar Cruiser, A Large, Deep Space Solar Sail. Breckenridge, Colorado, February 2023. AAS Guidance, Navigation and Control Conference. Paper AAS-23-117.